ON THE REDISTRIBUTION OF OB STAR LUMINOSITY AND THE WARMING OF NEARBY MOLECULAR CLOUDS

D. LEISAWITZ[1] AND M. G. HAUSER
Laboratory for Astronomy and Solar Physics, NASA Goddard Space Flight Center

ABSTRACT

IRAS observations of the neighborhoods of six H II regions in the outer Galaxy have been correlated with CO maps of the same regions. We find that more than half of the far-infrared luminosity from within ~ 25–75 pc of the ionizing stars is contributed by dust associated with molecular clouds; however, a major and temporally increasing fraction of the OB cluster starlight is not absorbed locally. These observations are consistent with what one would expect if the H II regions were not radiation-bounded and had ion densities ~ 1 cm^{-3}.

The radiated energy of open OB star clusters is found to be distributed in the interstellar medium in accordance with the solid angle subtended by molecular clouds at the cluster. This solid angle tends to decrease with increasing cluster age, as the clouds recede from the clusters. A model is proposed to describe the interstellar environment of OB star clusters as a function of time. It follows from this model that (*a*) the compact H II regions formed by massive stars when they are embedded in molecular clouds contribute at least as much of the Galaxy's warm dust luminosity as do more evolved H II regions; (*b*) massive stars contribute substantially to the Galaxy's interstellar radiation field and thus provide much of the energy required to heat dust throughout the Galactic disk, but a substantial fraction of the radiation may leak out of the Galactic dust layer; and (*c*) the far-infrared spectrum of a galaxy depends not only on its massive star number and formation rate, but sensitively on the relative duration of the compact H II region phase in its star-forming regions.

Subject headings: clusters: open — infrared: sources — interstellar: grains — nebulae: H II regions — radiative transfer — stars: early-type

I. INTRODUCTION

How one interprets the far-infrared (FIR) emission from the Galaxy and from other spiral galaxies depends on one's knowledge of what supplies the energy to heat interstellar dust grains, and how the energy is distributed among grains in the various gaseous components of the interstellar medium. The observed strong correlations of FIR luminosity with radio continuum luminosity and with other tracers of massive stars in spiral galaxies (see Soifer, Houck, and Neugebauer 1987 and references therein) are widely believed to imply that massive stars are largely responsible for heating the dust. But, as a rule, massive stars are concentrated in the arms of spiral galaxies and are accompanied by molecular clouds and diffuse atomic gas as well as ionized gas. Thus, the fraction of the FIR luminosity attributable to each of these gaseous phases is considerably less certain than is the source of luminosity itself.

A simple model of a volume of interstellar matter centered on a cluster of massive stars consists of a radiation-bounded sphere of ionized gas with accompanying dust which may be surrounded by an optically thick neutral cloud of uniform density. In a representative case, more than 60% of the stellar luminosity is absorbed and reradiated by dust in and around the ionized region (Natta and Panagia 1976). This model provides a reasonable description of the spectrum and brightness distribution of a compact H II region (see, e.g., Mezger and Wink 1975).

But a massive star spends a small part of its lifetime inside the molecular cloud from which it forms; probably more than

80% of all O stars are not embedded in their parental clouds (Mezger and Smith 1977). Once an OB star cluster breaks out of a molecular cloud, and an H II blister forms on the cloud's surface (Israel 1978), the cloud is accelerated (Leisawitz 1985), perhaps by strong stellar winds, and the radio and infrared brightness distributions of the region are drastically modified. Throughout this paper, we use the term blister H II region specifically to denote the interstellar environment of an ionizing star cluster after it has separated from its parental molecular cloud.

The Galaxy's infrared emission has been attributed primarily to dust in H II regions by some authors (e.g., Mezger, Mathis, and Panagia 1982; Cox, Krugel, and Mezger 1986; Cox and Mezger 1986) and to dust in molecular clouds by others (e.g., Fazio and Stecker 1976; Ryter and Puget 1977; Hauser et al. 1984b). Cox, Krugel, and Mezger (1986, hereafter CKM) and, more recently, Cox and Mezger (1986, hereafter CM) have analyzed FIR surveys of the Galaxy and concluded that "warm dust" associated with ionized gas in blister H II regions and "cold dust" heated only by the interstellar radiation field (ISRF) each contribute nearly half of the Galaxy's total FIR luminosity ($\sim 1.2 \times 10^{10}$ $L_\odot$; cf. Hauser et al. 1984b; Sodroski et al. 1987). In CM, the authors suggest that a galaxy's star formation rate (SFR) can be inferred from its total warm dust luminosity *if factors that affect the dust environment of stars can be understood* (one must know, as a function of time and of stellar mass, how much dust is near enough to a star to be heated to or above, say, 30 K). Alternatively, an empirical relation, obtained by dividing the Galactic SFR by its warm dust luminosity, is given by CM and one might assume that the ratio is applicable to observations of other galaxies.

[1] National Research Council Resident Research Associate.

To assume that a constant multiple of a measurable luminosity can yield a galaxy's star formation rate is appealing, but how reliable is this assumption? The relevant questions are: Where does the energy radiated by the massive stars that excite blister H II regions really go? What are the relative proportions of the locally absorbed starlight involved in heating dust associated with diffuse ionized gas, diffuse atomic gas, and molecular clouds? How do these functions change with time? The primary motivation of this paper is to address the first of these questions; some attention is also given to the others.

To address these questions, we have used *IRAS* observations at 12, 25, 60, and 100 μm and a survey of CO $J = 1 \rightarrow 0$ spectral line emission from the neighborhoods of open star clusters in the outer Galaxy (Leisawitz 1985; Leisawitz, Thaddeus, and Bash 1988, hereafter referred to as LTB). We present an analysis of six such regions, those surrounding star clusters NGC 7380, NGC 281, IC 1848, NGC 1624, NGC 1893, and NGC 2175. These systems are favorable for study since the distances and luminosities of these clusters are well known.

We find that most of the stellar luminosity is absorbed in the surrounding molecular material only in a relatively brief initial period following star formation. Thereafter, as the star and cloud separate, the majority of the infrared luminosity arises from the external surface of the remaining molecular material. The stars are surrounded by a very low density intercloud medium, and as the solid angle of molecular material exposed to the star becomes small, only a minor fraction of the total stellar luminosity is absorbed in the local environment.

The paper is organized as follows. The CO and infrared data are described in § II. In § III, the infrared background subtraction is discussed, and luminosities derived for the molecular clouds and for the entire stellar cluster neighborhoods are tabulated. Section IV contains an analysis of the density of the intercloud medium in the vicinity of the stellar clusters. A discussion of some implications of the results, in the framework of a model for the dynamic interstellar environment of OB stars, is presented in § V. Our results are summarized in § VI.

II. THE CO AND INFRARED DATA

The six regions studied lie outside the solar circle, where a molecular cloud can be associated with an H II region without ambiguity (i.e., confusion with unassociated clouds along the line of sight is not a problem and clear evidence exists for the interaction of the clouds with the visible nebulae) and the Galactic infrared background is relatively uncomplicated. We believe that this sample of star clusters is typical of regions in the blister H II phase (i.e., after the massive stars have broken out of their molecular clouds). In Table 1 are listed the star cluster coordinates (Alter, Ruprecht, and Vanysek 1970) and

distances, and the angular and linear radii of the regions analyzed.

Observations of ^{12}CO $J = 1 \rightarrow 0$ emission were obtained with the Columbia University 1.2 m millimeter wave telescope (LTB). The antenna beamwidth is 8.7 and the velocity resolution of the spectrometer is 0.65 km s^{-1}. The rms baseline noise in all spectra is $T_A{}^* \sim 0.28$ K. For each source, a circular region centered on the star cluster coordinates of the size indicated in Table 1 was mapped with a uniform sampling interval of 7.5. In each case, CO emission was mapped in a region of radius at least ~ 25 pc at the distance of the OB star cluster. A total of ~ 1400 spectra comprise the CO survey of the six regions considered here.

Molecular clouds were defined as features in the CO emission that are contiguous in both spatial and velocity coordinates. A catalog and maps of the molecular clouds in the six regions of interest are given by LTB.

Maps of 12, 25, 60, and 100 μm emission for each of the six regions were extracted from the *IRAS* Sky Flux images (*IRAS Catalogs and Atlases Explanatory Supplement* 1984). The images were taken from *IRAS* hours-confirmed (HCON) coverages 1 or 3 depending on which provided complete coverage of the region. The spatial resolution of the *IRAS* images, 4'–6', is modestly better than that of our CO observations.

III. INFRARED BACKGROUND SUBTRACTION AND LUMINOSITY CALCULATIONS

Our objectives were to determine (*a*) the fraction of the luminosity of the stars exciting the H II regions that is absorbed by nearby dust grains and reradiated in the infrared, and (*b*) the division of the infrared luminosity between grains associated with the molecular and nonmolecular gas components. To achieve these objectives, it is necessary to differentiate between source-related emission and background emission, to subtract the background emission component, and to extrapolate the *IRAS* luminosity to a bolometric infrared luminosity. Table 2*a* shows the mean brightness of each of the analyzed regions as observed by the *IRAS* (i.e., prior to background removal).

a) IR Emission from Dust in the Cluster Neighborhoods

In order to distinguish between source-related and background emission, one could imagine attributing to each star cluster a "sphere of influence" such that a dust grain at the surface of the sphere would be heated as much by the ISRF as by the cluster's starlight. The radius of such a sphere of influence should be about

$$r_s \approx [L_{cl}/4\pi c U_{ISRF}]^{0.5} ,$$

TABLE 1
ANALYZED REGIONS

STAR CLUSTER	H II REGION	GALACTIC (l, b) (deg)	COORDINATES (deg)	d^a (kpc)	REGION (deg)	RADIUS (pc)
NGC 7380	S142	107.08	−0.90	3.60	1.06	67
NGC 281	S184	123.13	−6.24	1.66	0.81	24
IC 1848	W5; S199	137.19	+0.92	2.31	1.06	43
NGC 1624	S212	155.35	+2.58	6.00	0.56	59
NGC 1893	IC 410; S236	173.59	−1.70	4.00	1.06	74
NGC 2175	S252	190.20	+0.42	1.95	1.56	53

^{a} References for distance: NGC 7380, IC 1848, NGC 1893, and NGC 2175 from Lyngå (1981), NGC 281 from Walker and Hodge (1968), and NGC 1624 from Moffat, FitzGerald, and Jackson (1979).

TABLE 2A

MEAN OBSERVED INFRARED INTENSITY (MJy sr^{-1}) OF ANALYZED REGIONS

Region	HCON[a]	N_{tot}[b]	12 μm	25 μm	60 μm	100 μm
NGC 7380	3	3690	15.7	30.0	26.6	82.1
NGC 281	3	2340	15.7	31.6	19.5	41.1
IC 1848	3	3370	20.2	38.7	56.8	144.0
NGC 1624	1	1310	28.6	54.2	21.7	43.5
NGC 1893	1	3760	41.1	81.5	38.6	57.5
NGC 2175	3	7610	36.0	75.7	40.3	74.8

[a] HCON denotes which IRAS hours-confirmed coverage was used. HCON 3 data were from the original release of HCON 3 images.

[b] N_{tot} is the number of 2' × 2' pixels over which the observed brightness is averaged.

TABLE 2B

DIFFUSE INFRARED BACKGROUND INTENSITY (MJy sr^{-1})[a]

Region	12 μm	25 μm	60 μm	100 μm
NGC 7380	15.0 (0.5)	28.5 (0.5)	19.0 (1.0)	60.0 (4.0)
NGC 281	15.2 (0.3)	30.5 (0.5)	11.5 (1.0)	22.0 (3.0)
IC 1848	17.5 (0.5)	34.5 (0.5)	22.0 (1.0)	65.0 (5.0)
NGC 1624	28.3 (1.0)	53.0 (1.0)	19.2 (0.4)	36.0 (5.0)
NGC 1893	40.7 (0.2)	80.5 (1.5)	31.0 (2.5)	39.0 (5.0)
NGC 2175	34.8 (0.2)	74.3 (0.6)	30.0 (0.8)	38.0 (5.0)

[a] Numbers in parentheses are 1 σ uncertainties.

where L_{cl} is the cluster luminosity and U_{ISRF} is the energy density of the interstellar radiation field. If $U_{ISRF} \approx 7 \times 10^{-13}$ ergs cm^{-3} (Keene 1981; Mathis, Mezger, and Panagia 1983), then $r_s \sim 40$ pc for a typical open cluster with O stars. In practice, r_s may be overestimated somewhat by equation (1) because the starlight is attenuated by gas and dust in and around an H II region. Thus, we have assumed that within the regions mapped in CO the measured IRAS intensity is the sum of source-related and background components, but that at projected radii not much greater than those of the mapped regions, only the background emission is seen. The terminology used in this paper to refer to dust associated with various constituents of the interstellar medium is illustrated in Figure 1.

The IRAS images contain as background both a zodiacal emission component and a diffuse galactic component. The zodiacal spectrum peaks in the IRAS 25 μm band and contributes relatively little at 100 μm (Hauser et al. 1984a). The diffuse galactic emission spectrum is characterized by a nearly constant 60 μm/100 μm intensity ratio of 0.25 in the galactic plane (Sodroski et al. 1987) and contributes relatively little to the observed 12 μm intensities. Unfortunately, the background levels are high: for a typical one of our regions, the source contributes $\sim 25\%-50\%$ of the measured mean brightness at 60 and 100 μm and less than 10% of the measured mean brightness at 12 and 25 μm. Accordingly, uncertainty in estimation of the background levels accounts for most of the uncertainty in the derived source luminosity.
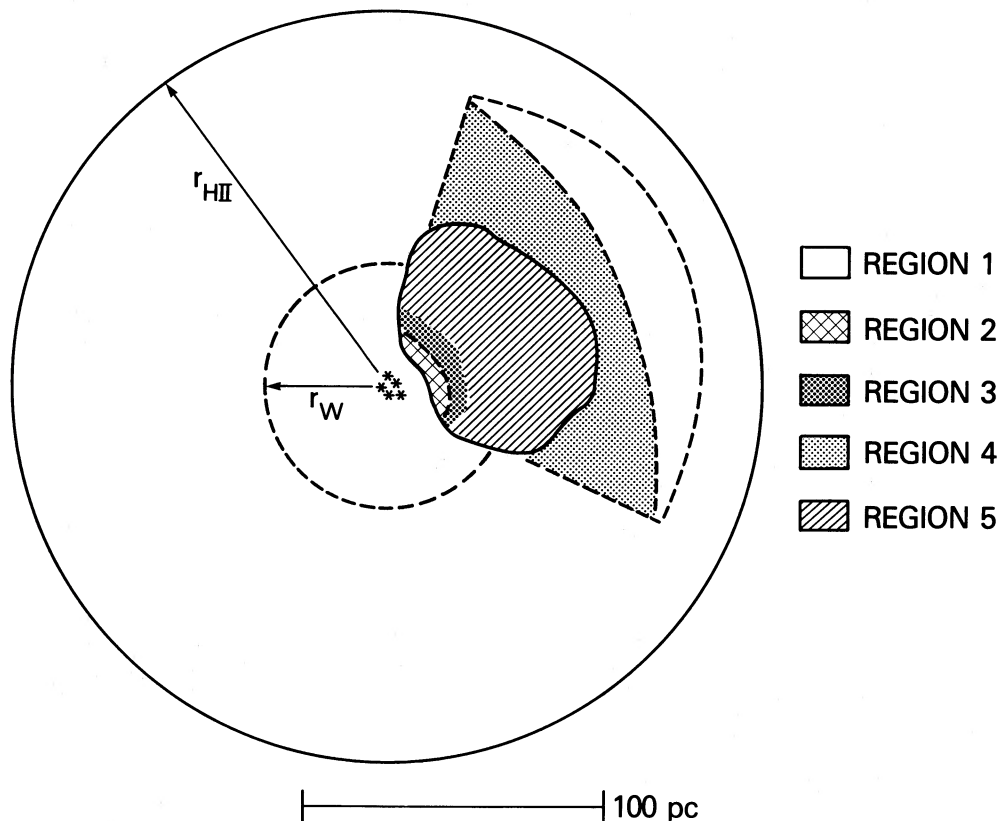

FIG. 1.—Two typical lines of sight toward an open OB star cluster neighborhood. Line of sight A intersects only the low-density, ionized region near the cluster; B intersects a molecular cloud illuminated by the cluster. The "sphere of influence" radius (eq. [1]), r_s, is shown. Background infrared radiation comes from interplanetary dust and dust in the Galactic plane in front of and behind the cluster neighborhood. Source-related, or "local," emission comes from dust heated by the cluster.

To estimate, for each region considered, the combined galactic and zodiacal background levels at 12, 25, 60, and 100 μm, we examined 16° long profiles of *IRAS* intensity versus galactic latitude at a series of at least three constant longitudes. One profile was at the longitude of the source; the others were at nearby longitudes, did not intersect the region mapped in CO, and did not cross the path of a discrete source near the latitude of the mapped region. A constant background level and associated uncertainty were estimated from the latitude profiles (Table 2B). Quoted uncertainties are conservative estimates that take into account pixel-to-pixel variations and uncertainties due to gradients that sometimes exist across the regions of interest.

The dust luminosity is proportional to the average source intensity from the emitting region. In-band source luminosities were derived from

$$L_i(L_\odot) \approx 0.11 d_{\text{kpc}}^2 N\langle I_\nu\rangle_i \Delta\nu_i(10^{12}\ \text{Hz})\,, \qquad (1)$$

for $i = 12$, 25, 60, and 100 μm, where $\langle I_\nu\rangle$ is the mean flux density per unit solid angle (MJy sr^{-1}) from the emitting region that subtends $N\ 2' \times 2'$ pixels, d_{kpc} is the source distance in kpc, and $\Delta\nu$ is the effective bandwidth. The effective 12, 25, 60, and 100 μm bandwidths are, respectively, 17.8, 6.17, 2.75, and 0.954 THz (*IRAS Catalogs and Atlases Explanatory Supplement* 1984). The bolometric luminosity (Lonsdale et al. 1985) was derived from

$$L_{\text{bol}}(L_\odot) \approx 1.73[L_{60\,\mu\text{m}} + L_{100\,\mu\text{m}}]\,. \qquad (3)$$

Note that the bolometric luminosity estimate does not explicitly include the measured 12 and 25 μm intensities, even though these intensities lie somewhat above a single-temperature fit to the 60 and 100 μm data. We have chosen to ignore this contribution partly because it is relatively small (typically $\lesssim 10\%$ of the quoted L_{tot}), and partly because it is poorly determined. Inclusion of this contribution would not impact our principal conclusions. Since equation (3) is accurate to within $\sim 10\%$ for regions in which I_{60}/I_{100} is in the range ~ 0.3–1.3 (cf. Appendix B of Lonsdale et al. 1985), no further bolometric corrections were made to account for very hot or very cold dust; equation (3) is applicable to all of the situations that we shall consider (see Table 2).

Using the distances from Table 1, and the total and background intensity levels from Table 2, we calculated source luminosities for each of the six regions (Table 3). Uncertainties tabulated for bolometric luminosities include the 10% uncertainty introduced by applying equation (3) as well as the background level uncertainties. We have not included the uncertainties inherent in the *IRAS* photometric calibration or source distance estimates.

In Table 4, we compare the bolometric IR luminosities of the cluster neighborhoods (L_{tot}) with the cluster luminosities. The cluster luminosities can be approximated as the sum of the luminosities of the O and early B spectral type stars. In most cases, $L_{\text{tot}} \ll L_{\text{OB}}$. Evidently, *a large fraction of the cluster starlight is not absorbed by dust grains within the regions examined.* If many low-mass stars are present in addition to the O and B stars, the cluster luminosities could be somewhat higher, thus strengthening this conclusion. Since distance uncertainties affect L_{tot} but not L_{OB}, the ratios in Table 4 are uncertain by $\sim 30\%$ due to this cause alone (LTB). Systematic errors in the calibration of *IRAS* data are believed to be too small to affect the conclusion. Note that the infrared to stellar luminosity

TABLE 3
TOTAL IR LUMINOSITIES OF H II REGION NEIGHBORHOODS ($10^3\ L_\odot$)[a]

Region	$L_{12\,\mu\text{m}}$	$L_{25\,\mu\text{m}}$	$L_{60\,\mu\text{m}}$	$L_{100\,\mu\text{m}}$	L_{tot}[b]
NGC 7380	54 (41)	42 (16)	109 (21)	110 (24)	359 (54)
NGC 281	5.3 (3.5)	4.2 (2.2)	15 (2.9)	13 (2.7)	46 (6.5)
IC 1848	78 (16)	44 (6.3)	182 (9.1)	153 (13)	548 (58)
NGC 1624	24 (82)	33 (30)	34 (11)	36 (27)	115 (44)
NGC 1893	39 (22)	36 (56)	135 (50)	114 (34)	407 (96)
NGC 2175	56 (11)	24 (12)	90 (12)	110 (18)	331 (44)

[a] Numbers in parentheses are 1 σ uncertainties not including distance or *IRAS* calibration uncertainties.

[b] L_{tot} is the bolometric luminosity of the region from eq. (3).

ratios would have been even smaller had molecular clouds been absent from the regions studied, since the clouds are opaque to the stellar radiation and transparent in the FIR regime. An exception to the trend that $L_{\text{tot}}/L_{\text{OB}} \ll 1$ occurs for the NGC 2175 region: there the surface filling factor of molecular clouds in the plane of the sky is ~ 1, and we measure $L_{\text{tot}} \sim L_{\text{OB}}$. IC 1848 is an intermediate case.

b) IR Emission from Dust Associated with Molecular Clouds

Qualitative evidence suggests that the molecular clouds near OB clusters are the major source of local cluster-induced infrared luminosity. Quantitative analysis of these regions, discussed below, confirms this conclusion. Figure 2 (Plate 7) shows $\Sigma[I_\nu \Delta\nu]_i$ summed for the 60 and 100 μm *IRAS* bands (cf. eq. [3]) and I_{60}/I_{100} maps of the regions surrounding IC 1848 and NGC 281. The maps showing $\Sigma[I_\nu \Delta\nu]_i$ indicate the spatial distribution of infrared "bolometric" surface brightness, while the I_{60}/I_{100} ratio maps illustrate approximately dust temperature variations. Also shown are the same regions of the sky as seen on the Palomar Observatory Sky Survey (POSS) prints. It is evident in these two cases that more of the infrared luminosity is contributed by dust near the molecular clouds than by dust in the low-density H II regions.

In order to isolate the infrared luminosity of the molecular clouds associated with our six H II regions, we considered that, in addition to diffuse background emission from interplanetary and foreground and background galactic dust, a potentially substantial contribution to the infrared emission along the line of sight might be made by dust near the illuminating star clus-

TABLE 4
FRACTION OF CLUSTER STARLIGHT ABSORBED LOCALLY BY DUST

Region	L_{OB}[a] ($10^3\ L_\odot$)	References for Cluster OB Stars	$L_{\text{tot}}/L_{\text{OB}}$
NGC 7380	1600	Moffat 1971; Israel 1977	0.22
NGC 281	630	Georgelin 1975; Israel 1977	0.073
IC 1848	970	Cruz-Gonzales et al. 1974	0.55
NGC 1624	600	Moffat et al. 1979	0.19
NGC 1893	2400	Moffat 1972; Mermilliod 1976	0.17
NGC 2175	300	Grasdalen and Carrasco 1975	1.10[b]

[a] Stellar luminosities are based on spectral types from cited references and stellar parameters tabulated by Panagia (1973).

[b] The H II region S247 is an additional $10^5\ L_\odot$ heat source (Georgelin 1975) for the dust in the region around NGC 2175. If the luminosity of the exciting stars in S247 had been included in L_{OB} then the ratio $L_{\text{tot}}/L_{\text{OB}}$ would be less than 1. In particular, S247 may dominate the heating of molecular cloud N2175A (LTB).
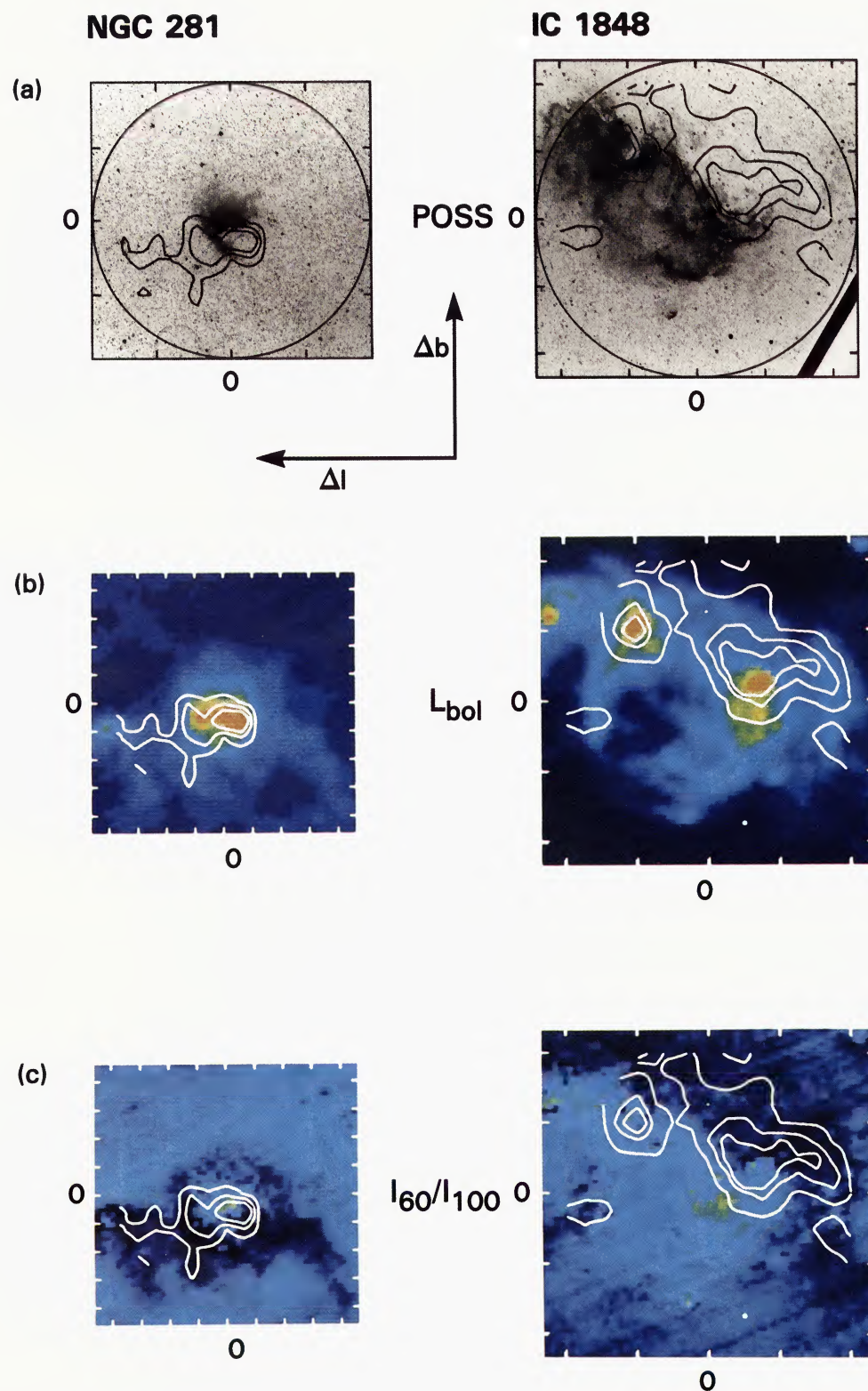
PLATE 7

NGC 281

IC 1848

FIG. 2.—Images of the regions around IC 1848 and NGC 281. Coordinates are relative to cluster positions (Table 1). (a) POSS print reproductions with overlays of CO intensity contours from LTB. For IC 1848: $\int T_A{}^*(CO)dv = 3, 10$, and 15 K km s^{-1} levels on red print; for NGC 281: 3, 6, and 9 K km s^{-1} levels on blue print. Circles delineate boundaries of regions mapped for CO emission. Tick marks are separated by $0°25$. (b) False color images of L_{bol} (see text) with CO contours superposed. (c) False color images of $IRAS$ 60 μm/100 μm intensity ratio with CO contours superposed.
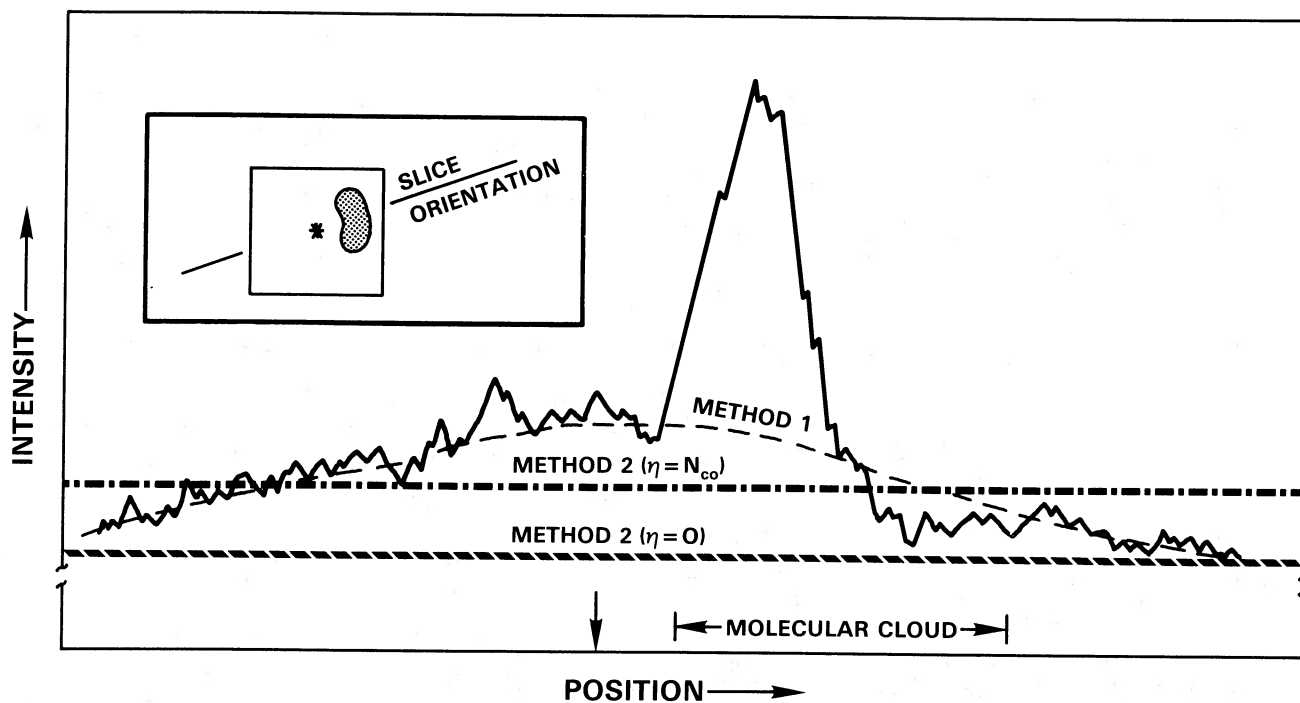
D. LEISAWITZ AND M. G. HAUSER (see **332**, 957)

Fig. 3.—Schematic illustration of IR background removal for molecular clouds near H II regions. Lines of sight with CO emission (stipled area in inset) are distinguished from lines of sight with no CO emission ($\overline{CO}$). Method 1: polynomial is fitted to IR intensity in $\overline{CO}$ region and subtracted from molecular cloud IR intensity. Method 2: constant IR intensity subtracted from molecular cloud intensity (parameter η described in text). Vertical arrow along abscissa marks position of OB cluster.

ters but outside the molecular clouds (see Fig. 1). Starting with maps from which the diffuse infrared background (Table 2B) had been subtracted, two methods were used to estimate and subtract the infrared emission due to dust near the star clusters; the methods are illustrated schematically in Figure 3. This was done to assure that the measured cloud luminosities were not systematically in error by an amount that could alter our conclusions. Shadowing of one molecular cloud by another along a given line of sight did not pose a problem for any of the regions considered here.

In method 1, a mask was made for each cluster region to indicate those pixels in which molecular clouds or compact infrared sources were detected. Then a smoothly varying function (a polynomial of third order in the direction perpendicular to the galactic plane and second order in the direction parallel to the galactic plane) was fitted to the $IRAS$ intensities measured in unmasked pixels. This procedure was followed for each of the four $IRAS$ bands. A measure of the quality of each such local emission model is the standard deviation of the measured intensities in unmasked pixels from the model polynomial (Table 5). A large standard deviation, such as the one obtained for the 100 μm fit in the region around IC 1848, indicates that local infrared emission has a lot of structure on a scale smaller than the region modeled.

The fitted polynomials were then used as interpolating functions to estimate the local emission toward masked pixels, i.e., toward the molecular clouds. The difference between the (background corrected, § IIIa) $IRAS$ intensities and the interpolating function corresponds to emission from dust associated solely with the molecular clouds. Luminosities of the individual molecular clouds, calculated by applying equations (2) and (3) to regions inside the $\int T_A^*(^{12}CO)dv = 1$ K km s^{-1}

contour, are given in Table 6. Upper limits (3 σ) are tabulated for molecular clouds that do not stand out above the local dust emission. Uncertainties in the bolometric luminosities include the 10% uncertainty of equation (3) and the standard deviations from the local emission model (Table 5); uncertainties due to distance determination and the $IRAS$ calibration are not included.

Note that, although embedded heat sources apparently are present in some of the cataloged molecular clouds, the luminosities of those sources are insufficient to explain the cloud luminosities. A striking example of this is cloud IC 1848A, in which Wilking et al. (1984) have noted the presence of an embedded infrared source with a luminosity $\sim 4 \times 10^3$ $L_\odot$. The embedded source fails by a factor ~ 20 to explain the luminosity that we measure for the entire cloud.

If a molecular cloud is large compared to r_s (eq. [1]), then the local noncloud infrared emission will be overestimated because emission from dust adjacent to the cloud will be greater than emission from dust in nonmolecular gas along the line of sight

TABLE 5

STANDARD DEVIATIONS (MJy sr^{-1}) FROM SMOOTH LOCAL EMISSION MODELS (Method 1)

Region	12 μm	25 μm	60 μm	100 μm
NGC 7380	0.48	0.73	4.7	12.0
NGC 281	0.42	0.67	3.6	7.9
IC 1848	0.99	6.9	14.0	31.0
NGC 1624	0.29	0.48	0.88	3.3
NGC 1893	0.51	1.0	5.8	13.0
NGC 2175	0.64	1.7	1.3	5.6

TABLE 6

LUMINOSITIES OF MOLECULAR CLOUDS (L_{mol}) FROM METHOD 1 ($10^3 L_\odot$)

Cloud[a]	$L_{12\,\mu m}$	$L_{25\,\mu m}$	$L_{60\,\mu m}$	$L_{100\,\mu m}$	L_{bol}[b]	
N7380A	<0.52	<0.29	<0.93	<0.82	<2.9	
N7380B	<0.02	<0.26	<0.84	<0.78	<2.6	
N7380C	<0.35	<0.20	<0.62	<0.57	<1.9	
N7380D	3.7	1.0	<1.0	4.3	8.4	(1.4)
N7380E	22	19	61	41	167	(17)
N281A	3.4	2.6	9.5	6.8	27	(2.7)
IC1848A	24	39	22	28	82	(8.5)
IC1848B	12	7.1	26	23	81	(8.2)
IC1848C	1.3	<0.68	<0.66	0.54	0.93	(0.65)
IC1848E	0.54	0.90	0.76	0.29	1.7	(0.68)
N1624A	<0.59	<0.36	<0.35	0.32	0.55	(0.43)
N1624B	11	9.5	25	18	71	(7.1)
N1893A	19	19	65	42	173	(17)
N1893B	<0.20	<0.14	<0.43	<0.32	<1.2	
N1893C	3.5	1.3	5.7	4.5	17	(1.9)
N1893D	<0.30	<0.22	<0.66	<0.49	<1.9	
N1893E	<0.40	<0.30	<0.86	<0.66	<2.5	
N2175A	8.6	9.4	19	16	57	(5.7)
N2175B	27	20	56	48	171	(17)
N2175C	1.0	0.72	0.63	1.2	3.1	(0.33)
N2175D	<0.10	<0.10	<0.04	<0.06	<0.17	
N2175E	2.2	0.86	1.1	2.0	5.2	(0.53)
N2175F	<0.26	2.0	0.54	1.2	2.8	(0.31)
N2175G	13	6.5	5.3	10	26	(2.6)

[a] Cloud names are those of LTB. Only clouds that are likely to be associated with the H II regions are analyzed here.
[b] Numbers in parentheses are 1 σ uncertainties. Upper limits are 3 σ.

to the cloud. In such a case, the cloud luminosity will be underestimated. This is likely to have affected our estimates of the luminosities of the large clouds found near IC 1848 and NGC 2175.

A more straightforward way than method 1 to derive the IR emission of just the molecular clouds in a region is to subtract a constant equal to the average intensity measured along lines of sight toward which no CO emission was detected. This was our second method (method 2).

An advantage that method 2 has over method 1 is the relative ease with which the fraction, f_{mol}, of the total luminosity from a region contributed by molecular clouds can be computed:

$$f_{mol} \equiv L_{mol}/L_{tot} \approx 1 - [1 + \eta/N_{\overline{CO}}][L_{\overline{CO}}/L_{tot}] , \qquad (4)$$

where L_{tot} (Table 3) is the bolometric infrared luminosity from all pixels, N_{tot} (Table 2A), within the mapped region; $L_{\overline{CO}}$ is the infrared luminosity from $N_{\overline{CO}}$ pixels, in the directions of which no CO emission was detected.

In equation (4), η is a number ranging from 0 to the number of pixels, N_{CO}, in which CO emission was observed ($N_{CO} \equiv N_{tot} - N_{\overline{CO}}$). Taking $\eta = 0$ corresponds to the case of removing no emission by dust in the vicinity of the H II region from lines of sight containing CO emission. The case $\eta = 0$ might be applicable for regions in which the size of a molecular cloud is not much smaller than the size of the cluster's sphere of influence (e.g., IC 1848 and NGC 2175). If η is taken to be equal to N_{CO}, then a local emission with intensity the same as the average value in the "$\overline{CO}$" pixels is subtracted from lines of sight toward the molecular clouds. Method 1 is more closely approximated by the case $\eta = N_{CO}$ since, in that method, the background contributed by dust near the illuminating stars is

TABLE 7

FRACTION OF LUMINOSITY CONTRIBUTED BY MOLECULAR CLOUDS (f_{mol})

REGION	METHOD 1	METHOD 2[a]	
		$\eta = N_{CO}$	$\eta = 0$
NGC 7380	0.49 (0.09)	0.57 (0.10)	0.79 (0.15)
NGC 281	0.59 (0.10)	0.70 (0.12)	0.83 (0.15)
IC 1848	0.31 (0.05)	0.54 (0.08)	0.79 (0.12)
NGC 1624	0.62 (0.25)	0.78 (0.31)	0.92 (0.43)
NGC 1893	0.47 (0.12)	0.52 (0.13)	0.64 (0.17)
NGC 2175	0.80 (0.13)	0.79 (0.17)	0.97 (0.18)

[a] Parameter η is defined in the text (see eq. [4]).

modeled and subtracted from the lines of sight containing the clouds (see Fig. 3).

Values of f_{mol}, in the two limiting cases $\eta = 0$ and $\eta = N_{CO}$, are given for each of our six regions in Table 7. Also tabulated are the corresponding fractions derived by dividing the sum of the cloud luminosities calculated with method 1 by the total region luminosities (Table 3). Method 1 tends to yield $\sim 10\%$ lower molecular cloud luminosities than method 2 with $\eta = N_{CO}$. This occurs because the shapes of the polynomials in method 1 are such that the average IR intensity subtracted as local noncloud emission is greater than the average intensity observed toward "$\overline{CO}$" pixel directions (see Fig. 3), and because a small amount of CO emission occurs along lines of sight outside the cloud boundaries adopted for method 1. The real fraction of the infrared luminosity contributed by molecular clouds to each of the regions described in Table 1 probably is a number that lies between a lower limit derived with method 1 and an upper limit derived with method 2 when η is taken to be zero. This is because the emission contributed by dust near the illuminating stars to lines of sight toward the molecular clouds may be overestimated by the former method and must be underestimated by the latter.

The quantitative analysis summarized in Table 7 suggests that *most of the IR luminosity of the H II region neighborhoods studied is contributed by dust associated with molecular clouds.* The self-consistency of our results from region to region and the values of f_{mol} derived for cases in which IR emission from the nebula is not confused with emission from dust in the clouds (e.g., NGC 281) support this conclusion.

To judge whether confusion between overlapping ionized and molecular regions could have caused a serious error in our finding that the molecular clouds, rather than the low-density ionized regions, are the source of most of the IR luminosity, we have examined the IC 1848 and NGC 281 regions in greater detail than the others. Radio continuum observations of the IC 1848 and NGC 281 regions, with spatial resolution comparable to that of the CO and *IRAS* data, have been made by Vallee, Hughes, and Viner (1979) and Roger and Pedlar (1981). While low-level radio continuum contours are similar in extent to the regions of visible nebulosity, the strongest radio emission comes from directions in which the molecular clouds interface with the low-density, ionized gas (region 2 in Fig. 4). Indeed, it is near these interface regions that the strongest infrared emission occurs (regions 2 and 3 in Fig. 4; cf. Fig. 2). Despite the fact that the molecular clouds near IC 1848 and NGC 281 are receding from the OB star clusters at speeds of ~ 10–20 km s^{-1} (cluster velocities are from Wramdemark [1982] and Cruz-Gonzales et al. [1974] and CO velocities are
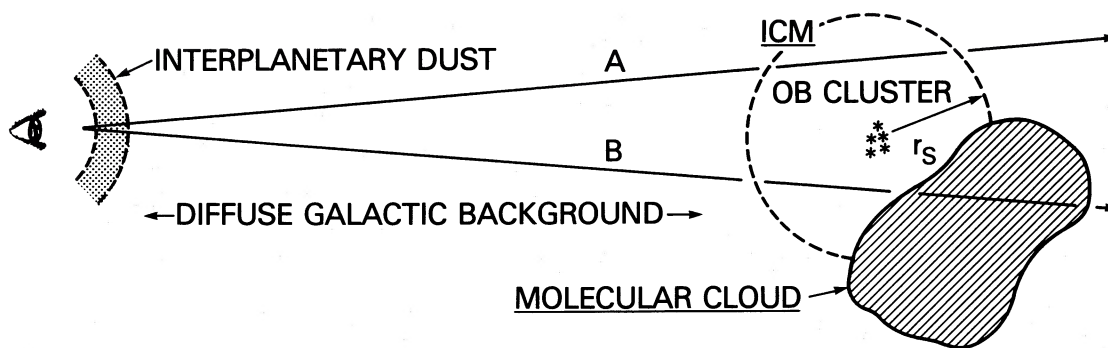
FIG. 4.—Interstellar components of a typical blister H II region. *Region 1*: ~ 1 cm^{-3} ionized ICM; r_{HII} is the radius of ionization. *Region 2*: dense, ionized gas and warm dust on molecular cloud surface. *Region 3*: warm dust heated by nonionizing photons. *Region 4*: cold ICM in shadow cast by molecular cloud. *Region 5*: cold interior of molecular cloud, opaque to OB cluster UV radiation. Dust interior to some radius, r_w, is "warm" but most energy radiated by cluster escapes to greater distance and contributes to "cold" (cirrus) component of galactic IR emission.

from LTB), radio recombination line observations (Hart and Pedlar 1976; Roger and Pedlar 1981) in the directions of the strong continuum emission show radial velocities for the *dense*, ionized gas within a few km s^{-1} of the CO velocities. Analogous behavior was found in the cases of all well-studied H II regions discussed by LTB. These observations are at least qualitatively consistent with a model in which the gas in molecular clouds associated with blister H II regions is being dissociated and ionized and dust on the surfaces of the molecular clouds is reponsible for most of the FIR luminosity coming from the H II region neighborhoods.

IV. DENSITY OF THE INTERCLOUD MEDIUM

We have found that infrared and CO observations of the regions around the star clusters NGC 7380, NGC 281, IC 1848, NGC 1624, NGC 1893, and NGC 2175 indicate that a minor fraction of the stellar luminosity is absorbed by dust grains in and around blister H II regions and that most of the starlight that is absorbed locally by dust is absorbed on the surfaces of nearby molecular clouds. These results would *not* have been expected if blister H II regions were essentially ionization-bounded spheres with electron density ~ 10 cm^{-3} and a "normal" dust-to-gas mass ratio of $\sim 10^{-2}$.

In Table 4 we compared the luminosities of the clusters with the measured infrared luminosities and found that, in general, $L_{tot} \ll L_{OB}$. Since molecular clouds are essentially opaque to most of the radiated stellar energy, this result can be explained only if the intercloud medium (ICM) in the observed regions (region 1 in Fig. 4) is optically thin to the starlight.

It is of interest to know the UV/optical linear absorption coefficient, α, for dust in the ICM near OB clusters since the linear absorption coefficient is proportional to the dust density. Consider a star of luminosity L_* embedded in a volume of dust of uniform density. In thermal equilibrium, which quickly obtains, the starlight absorbed within a spherical region of radius r is balanced by the infrared energy radiated by the dust in that sphere. If $\tau = \alpha r$ is the spectrally averaged dust opacity from the star to radius r and if $\tau \ll 1$, then the rate at which energy is absorbed is τL_*. Then, if we denote by $L_{IR}(r)$ the rate at which energy is emitted by the dust interior to r, the dust absorption coefficient is given by $\alpha \approx [L_{IR}(r)/L_*]r^{-1}$.

The infrared luminosity of the ICM in the vicinity of a star cluster can be taken to be $L_{tot}(1 - f_{mol})$, where L_{tot} is the total region infrared luminosity and f_{mol} is the fraction of this total

contributed by molecular clouds. Accordingly, the absorption coefficient is given approximately by

$$\alpha_{ICM} \approx (L_{tot}/L_{OB})(1 - f_{mol})r^{-1} . \quad (5)$$

Values for the ratio of infrared to stellar luminosity (Table 4) are combined with values for f_{mol} (Table 7) and the region radii (Table 1) to derive the values tabulated for α_{ICM} in Table 8.

Of course, equation (5) is only an approximation, because many of the characteristics of a real blister H II region, for example, the presence of shadows cast by molecular clouds (region 4 in Fig. 4) and absorption of ionizing photons by gas, have not been included.

Using radiative transfer models which incorporate such effects, we have obtained estimates for α_{ICM} which agree well with the values derived using equation (5). With the aid of these models, we estimate the uncertainty in α_{ICM} to be $\sim 30\%$ for blister H II regions in which the volume-filling factor of molecular clouds is not large. Since the volume-filling factors for the IC 1848 and NGC 2175 regions are large, we have excluded these regions in Table 8. In the remaining four regions, the absorption coefficients differ from each other by no more than the estimated uncertainty. The values range from 1.2 to 1.7×10^{-3} pc^{-1}, corresponding to dust opacities $\tau_{ICM} = \alpha_{ICM} r \lesssim 0.1$ for the analyzed regions (the region radii are given in Table 1).

A simple empirical expression can be derived for the constant of proportionality between the dust absorption coefficient and the gas density in the ICM. We use the ratio of total gas column density to $E(B-V)$ selective extinction measured by Bohlin, Savage, and Drake (1978), and use the interstellar extinction curve of Savage and Mathis (1979) to extrapolate $E(B-V)$ to ~ 1000 Å. It follows that the 1000 Å dust absorption coefficient,

$$\alpha(pc^{-1}) \approx 2.8 \times 10^{-3}[(1-A)/0.4]\delta n . \quad (6)$$

TABLE 8

MEASURED AND DERIVED PROPERTIES OF THE DIFFUSE INTERCLOUD MEDIUM

Region	α_{ICM} (pc^{-1})	τ_{ICM}	n_{ICM} (cm^{-3})	r_{HII} (pc)	EM (cm^{-6} pc)	T_B^{est} (K)	T_B^{obs} (K)
NGC 7380	0.0017	0.11	0.6	170	130	0.20	1.6
NGC 281	0.0013	0.03	0.5	150	66	0.10	0.5
NGC 1624	0.0012	0.07	0.4	160	58	0.09	0.6
NGC 1893	0.0012	0.09	0.4	240	88	0.14	0.5

Scattering of starlight by dust is an important factor in the normalization of the gas column density to extinction ratio, so we include the effect of grain albedo, A, and adopt 0.6 for the albedo at ~ 1000 Å (see Savage and Mathis [1979] and references therein; note that the theoretical calculations of White [1979] and Draine and Lee [1984] suggest that A could be as small as ~ 0.4). In equation (6), n is the mean gas density along a path through the interstellar medium (cm^{-3}), and the dimensionless factor δ represents a deficiency of dust relative to the "normal" dust-to-gas ratio ($\delta = 1$) from the Bohlin, Savage, and Drake (1978) calibration.

Our inferred values of α_{ICM} lead (for $\delta \sim 1$) to a gas density in the ICM of $n_{ICM} \sim 0.4$–0.6 cm^{-3}. This estimate for n_{ICM} agrees with, or may be slightly lower than, the mean gas density in the diffuse interstellar medium derivable from measurement of the $B-V$ color excess or visual extinction per kpc near the galactic plane (Münch 1952; Bohlin, Savage, and Drake 1978; Lyngå 1982). Ionized region radii, $r_{H II}$, and emission measures (EM $\sim 2 r_{H II} n_{ICM}^2$) corresponding to the stellar parameters and the derived ICM gas densities are also shown in Table 8 (cf. Table 2 of Reynolds and Ogden 1982). Dust absorption of ionizing radiation is taken into account in our calculation of the H II region radii (see Spitzer 1978). Comparison of Tables 8 and 1 shows that the intercloud medium is expected to be ionized to radii that are much larger than the radii of the regions analyzed.

The density estimates in Table 8 are also consistent with 1.4 GHz continuum measurements. In Table 8, model predictions are given for the 1.4 GHz continuum brightness temperature (T_B^{est}), proportional to the emission measure, for lines of sight that intersect only the ionized ICM in the studied regions. The 1.4 GHz survey of Reich (1982) is suitable for comparison with our calculations because low spatial frequency emission was not subtracted from the published contour maps. Although the brightness temperatures measured by Reich (T_B^{obs} in Table 8) are systematically higher than our predicted brightness temperatures, the measured and inferred values coincide to within $\sim 1 \sigma$ for the radio data (the principal source of uncertainty is in the absolute zero emission level) for three relatively isolated regions (NGC 281, NGC 1624, and NGC 1893). The systematic temperature difference may be attributable to the uncertain zero-point calibration or to sidelobe radiation from ionized surfaces of molecular clouds near the OB star clusters.

Our estimates for n_{ICM} are much lower than the density often considered to characterize blister H II regions, ~ 10 cm^{-3} (see, e.g., Mezger [1978] and references therein). To see how this difference can be reconciled, note that radio measurements of the emission measure may be dominated by emission from the relatively dense, heated surfaces of the molecular clouds in the cluster vicinity (see, e.g., Israel 1977; Israel 1978 and references therein; Roger and Pedlar 1981). This would bias the estimated mean electron density above that in the intercloud medium. In our regions, at least, it is only for lines of sight that intersect illuminated molecular cloud surfaces that the emission measure is relatively high, say greater than 10^4 cm^{-6} pc. We estimate that the depth of the layer that a typical OB star cluster could ionize at the surface of a nearby molecular cloud is of the order of 1 pc. The gas density obtained by dividing a typical observed emission measure by a path length as small as 1 pc, applicable to the case of a cloud with a heated surface seen face-on, is consistent with the mean hydrogen density greater than $\sim 10^2$ cm^{-3} inferred for molecular clouds from millimeter spectral line analyses. Thus, we suggest that the notion of a medium density (~ 10 cm^{-3}) sphere of ionized gas should be replaced with a picture of a generally low ($\lesssim 1$ cm^{-3}) density ionized medium containing thin but dense ionized layers on the illuminated surfaces of molecular clouds near the OB stars.

A potential alternative explanation for the small fraction of OB cluster infrared luminosity arising in the ICM would be that the dust-to-gas ratio in the ICM near OB clusters is anomalously low ($\delta \ll 1$). If one were to assume, for instance, that $\delta = 0.1$, then the inferred results in Table 8 would be modified systematically as follows: α_{ICM} and τ_{ICM} each would be unaffected since they are inferred from directly observed quantities (eq. [5]); the gas density, n_{ICM}, would become larger by a factor of 10 (eq. [6]); and the corresponding size of the region that a cluster could ionize ($r_{H II} \sim n^{-2/3}$) would shrink by more than a factor of 4.6. As a result of the change in n_{ICM} and $r_{H II}$, the emission measure predicted for a path through the ionized ICM would increase by a factor of 22. For the regions described in Table 8, at least, an emission measure as large as the one predicted for $\delta = 0.1$ is not consistent, by nearly an order of magnitude, with the 1.4 GHz map of Reich (1982). To explain the infrared *and* radio observations of the diffuse gas surrounding the OB clusters NGC 7380, NGC 281, NGC 1624, and NGC 1893, δ cannot be made much smaller than unity.

In summary, the low surface brightness of dust in the intercloud medium relative to the brightness of dust on the star-facing surfaces of molecular clouds near OB clusters (Fig. 2) is due to very low density gas in the ICM with nearly normal dust-to-gas mass ratio. The radio continuum surface brightness distribution is explained in a similar fashion. Generally, infrared intensity is determined by the distribution of dust grain temperature and column density along a line of sight through a source. Since even a molecular cloud of modest dimensions is sufficiently dense for its interior to be shielded from UV and visible photons, deeply embedded grains (region 5 in Fig. 4) are colder than grains near the cloud surface and in the surrounding ICM. This is reflected in the relatively cold color temperatures found along lines of sight toward which CO emission is detected near our star clusters (see Fig. 2c). Yet relatively high infrared intensities are found along these lines of sight. From this we infer that the dust density contrast between the molecular clouds and the ICM is large enough to offset the difference in dust temperature as far as the infrared intensity is concerned. A high-density contrast between the remnant molecular material and the intercloud medium would appear to explain the distribution of far-infrared and radio brightness surrounding young stellar clusters.

V. DISCUSSION

The above results, combined with the kinematics and morphology of the vicinities of young stellar clusters found by Leisawitz (1985; also see LTB), suggest the following scenario for the development of a blister H II region. An OB cluster forms a compact H II region inside a molecular cloud that is surrounded by diffuse atomic gas with a density ~ 1 H atom per cm^3. After only ~ 1 Myr, the cluster breaks out of the cloud because of a combination of stellar winds and a nearly 3 order of magnitude overpressure. The pressure is quickly relieved by expansion of the ionized region. Meanwhile, some mechanism, possibly stellar wind, accelerates what remains of the molecular cloud and maintains a low ICM density (cf. Elmegreen 1976). Stellar Lyman continuum photons impinging on the molecular cloud ionize a thin layer (~ 1 pc) of gas on its

surface, resulting in an ionized gas density of $\sim 10^2$ electrons per cm^3 and strong radio continuum emission that traces the cloud. Radio recombination and CO line measurements indicate that the freshly ionized gas flows away from the cloud and toward the low-density region closer to the stars at a few km s^{-1}. Some of the Lyman continuum photons and all of the nonionizing photons that encounter the molecular cloud heat dust grains near its surface, giving rise to strong infrared emission (in all four *IRAS* bands) that also traces the illuminated surface of the cloud. Only a small fraction (of the order of 10%) of the stellar luminosity that does not reach the surface of a nearby molecular cloud is absorbed in the local diffuse ICM. Hence, *the covering factor of molecular clouds, as seen from the illuminating cluster, is the primary determinant of the appearance of blister H II regions at both radio and infrared wavelengths, and of the ratio of bolometric IR luminosity to cluster luminosity.*

If the molecular clouds really are moving away from the stars as they appear to be (Leisawitz 1985), the radio and IR luminosities of blister H II regions should diminish rapidly as a function of the age of the region, approximately as t^{-2}. When a cluster first breaks out of a cloud, the IR luminosity should be comparable to that of the cluster. By the time a typical cloud reaches a distance ~ 20 pc from a cluster, absorption of the starlight occurs predominantly in the diffuse gas and the infrared to stellar luminosity ratio should asymptotically approach τ_{ICM} (see Table 8), the spectrally averaged opacity of the local ICM. Since the clouds move at ~ 10 km s^{-1} with respect to the stars, the length of the blister phase, during which the IR luminosity decreases, is only ~ 2 Myr. Since the lifetime of an O star is typically 5 Myr, the 2 Myr blister phase time scale is consistent with the observation by Torres-Peimbert, Lazcano-Araujo, and Peimbert (1974) that about half of all *visible* O stars are found outside dense H II regions.

Based on the analyses of Mezger and Smith (1976) and Torres-Peimbert, Lazcano-Araujo, and Peimbert (1974) we suppose that the star spends the first 20% of its lifetime freeing itself from the molecular cloud in which it formed (the compact H II region phase), the next 40% of its lifetime warming nearby cloud material (the blister phase), and the final 40% of its lifetime as a naked O star, with only $\sim 10\%$ or less of its starlight absorbed by nearby dust. A simple approximation for the fraction of OB cluster starlight converted to infrared luminosity within 50 pc of the stars might look like

$$f(t) \approx \begin{cases} 1.0 & \text{for} & t \lesssim 1 & \text{(compact phase)} \\ t^{-2} & \text{for} & 1 \lesssim t \lesssim 3 & \text{(blister phase)} \\ 0.1 & \text{for} & 3 \lesssim t \lesssim 5 & \text{(naked phase)} , \end{cases} \tag{7}$$

where t is in Myr. Since the integral of the starlight redistribution function, $\int f(t)dt/5$ Myr $= 0.37$, roughly 37% of an OB cluster's total radiated energy can be expected to be absorbed by nearby dust grains. Note that 1.2 times as much starlight is converted to IR near the stars during the compact phase than during the remainder of an O star's short lifetime.

The conclusion that only a minor fraction of OB cluster total energy output is reradiated in the infrared by dust near the stars is in contradiction to the interpretation of CM and CKM. This discrepancy would appear to arise because these authors treat blister H II regions (which they refer to as extended low-density, or ELD, regions) as radiation-bounded ionized regions in which the intrinsic dust absorption is $A_V \sim$

0.3 mag (corresponding to $\tau \gtrsim 1$ at UV wavelengths), whereas we find that $\tau_{ICM} \ll 1$ in the intercloud medium in the regions studied.

An important consequence of the low intercloud medium density inferred from our measurements and equation (5) is that the ionized regions surrounding OB clusters may be larger than 100 pc in radius (see Table 8 and Fig. 4). This is much larger (by at least a factor of 10) than the sort of region described by the ELD models of CKM. From this it follows that (a) the ionized ICM around OB clusters fills a large fraction of the volume of the galactic molecular cloud layer and therefore can be the source of the diffuse, low-level radio continuum background emission from the galactic plane (cf. Mezger 1978; Reynolds 1984), and (b) an appreciable fraction of the Lyman continuum photons radiated by the stars may escape from the galactic plane, since the expected diameters of the ionized regions are larger than the 120 pc thickness of the galactic molecular cloud layer (see, e.g., Dame 1983).

Our model for the redistribution of OB star luminosity in the local cluster environment can be used with an estimate of the total number of OB clusters in the Galaxy to predict the contribution made by OB cluster neighborhoods to the total Galactic infrared emission. To estimate the total luminosity of Galactic OB clusters we note that the clusters in our sample are characterized by a Lyman continuum photon production rate per unit OB star luminosity $\sim 3 \times 10^{43}$ s^{-1} $L_\odot^{-1}$ (using the stellar parameters of Panagia 1973) and that the total Galactic Lyman continuum photon production rate, from radio observations, is $\sim 3 \times 10^{53}$ s^{-1} (Gusten and Mezger 1982). It follows that the Galaxy's OB cluster luminosity is $\sim 10^{10}$ $L_\odot$. In fact, the integrated OB cluster luminosity may be somewhat greater than 10^{10} $L_\odot$ for two reasons. Gusten and Mezger made the simplifying assumption that no Lyman continuum photons escape from blister H II regions (or naked O stars) and leave the Galaxy. But the ICM opacity inferred from our analysis of infrared data suggests that blister H II regions could leak ionizing photons in which case radio continuum survey data would lead to an underestimate of the galactic Lyman continuum photon production rate. Furthermore, OB clusters generally contain some low-mass stars that contribute to the luminosity but not to the ionizing photon flux. We have already seen (eq. [7]) that $\sim 37\%$ of an average OB cluster's total radiated energy can be expected to be absorbed by dust grains within ~ 50 pc of the stars. Thus, greater than $\sim 4 \times 10^9$ $L_\odot$ should be converted to IR luminosity in the cluster neighborhoods according to our model. This number agrees well with the "warm" dust luminosity of the Galaxy, 6×10^9 $L_\odot$, derived by CM from the *IRAS* and other infrared surveys of the Galactic plane.

Since as much as 63% of the OB cluster luminosity, the fraction *not* absorbed within the cluster neighborhood, can heat dust outside the local cluster environment, an additional 6×10^9 $L_\odot$ contribution to the total Galactic infrared emission can be made by OB clusters. This contribution, however, is sensitive to the fraction of cluster photons that escape from the Galactic dust layer due to the large sizes of the low-density H II regions (cf. Helou 1986; Lonsdale, Persson, and Helou 1987).

We now return to the central question: can a galaxy's warm dust luminosity yield a reliable estimate of its content of massive stars and star formation rate? Such an argument requires one to assume that there is little variation from galaxy to galaxy in the way that OB cluster starlight is converted to

infrared luminosity. The *form* of our model for the redistribution of OB cluster starlight in the interstellar medium may well be galaxy-independent. This would be true if the physical mechanisms that operate to end the compact H II region phase and to accelerate molecular clouds are the same elsewhere as in the regions that we have studied. However, the *parameters* to which our model is most sensitive, namely the time scales that determine the relative durations of the "compact" and "blister" phases, may not be constant from galaxy to galaxy. For example, since the stellar initial mass function may be affected by the metallicity of the interstellar medium, the H II region phase time scales may be metallicity-dependent. Thus, even H II regions in the inner Galaxy, where the metallicity is higher than it is in the solar neighborhood, may differ from the regions considered here. Furthermore, variations in the dust layer thickness should be expected to affect the fraction of OB cluster radiation that is not absorbed locally, the so-called "cirrus" or "cold" component of a galaxy's infrared spectrum.

VI. SUMMARY

We have analyzed *IRAS* 12, 25, 60, and 100 μm maps of regions surrounding six OB star clusters. The clusters are in blister H II regions. Components of a typical blister H II region are illustrated schematically in Figure 4. We find that:

1. the total FIR luminosity from dust heated by the cluster stars (within ~ 25–75 pc) is typically a small fraction (~ 0.2) of the cluster luminosity, but can be higher in regions in which molecular clouds subtend a large solid angle at the cluster; and

2. of the locally absorbed starlight, most ($\sim 50\%$–80%) is radiated by dust near the illuminated surfaces of molecular clouds associated with the young clusters.

These observational results can be understood in terms of a model for blister H II regions in which the stars reside in a very low density ($\lesssim 1$ cm^{-3}) intercloud medium and nearby molecular clouds are the primary local absorbers of starlight. The UV/visible radiation from the stars ionizes gas and warms dust near the surfaces of the clouds, accounting for the observed strong radio continuum and infrared emission from lines of sight toward these heated surfaces. By comparison, the infrared and radio continuum intensities from lines of sight that intersect only the intercloud medium are faint. The intercloud medium is ionized to a radius greater than 100 pc from the OB stars.

Since molecular clouds recede from OB clusters at ~ 10 km s^{-1}, the blister phase endures for only ~ 2 Myr and probably contributes much less to the Galaxy's "warm dust" luminosity than the phase during which the O stars are surrounded by dense molecular material. Massive stars contribute substantially to the Galaxy's "cold dust" luminosity after they break out of the clouds in which they form.

REFERENCES

Alter, G., Ruprecht, J., and Vanysek, V. 1970, *The Catalog of Star Clusters and Associations* (Budapest: Akademia Kiado).
Bohlin, R. C., Savage, B. D., and Drake, J. F. 1978, *Ap. J.*, **224**, 132.
Cox, P., Krugel, E., and Mezger, P. G. 1986, *Astr. Ap.*, **155**, 380 (CKM).
Cox, P., and Mezger, P. G. 1986, in *Star Formation in Galaxies*, ed. C. J. Lonsdale Persson (NASA CP-2466), p. 23 (CM).
Cruz-Gonzales, C., Recillas-Cruz, E., Costero, R., Peimbert, M., and Torres-Peimbert, S. 1974, *Rev. Mex. Astr. Ap.*, **1**, 211.
Dame, T. M. 1983, Ph.D. thesis, Columbia University (published as NASA Tech. Paper 2288).
Draine, B. T., and Lee, H. M. 1984, *Ap. J.*, **285**, 89.
Elmegreen, B. G. 1976, *Ap. J.*, **205**, 405.
Fazio, G. G., and Stecker, F. W. 1976, *Ap. J. (Letters)*, **207**, L49.
Georgelin, Y. M. 1975, Ph.D. thesis, Université de Provence Marseille.
Grasdalen, G. L., and Carrasco, L. 1975, *Astr. Ap.*, **43**, 259.
Gusten, R., and Mezger, P. G. 1982, *Vistas Astr.*, **26**, 159.
Hart, L., and Pedlar, A. 1976, *M.N.R.A.S.*, **176**, 135.
Hauser, M. G., *et al.* 1984a, *Ap. J. (Letters)*, **278**, L15.
Hauser, M. G., Silverberg, R. F., Stier, M. T., Kelsall, T., Gezari, D. Y., Dwek, E., Walser, D., and Mather, J. C. 1984b, *Ap. J.*, **285**, 74.
Helou, G. 1986, *Ap. J. (Letters)*, **311**, L33.
IRAS Catalogs and Atlases, Explanatory Supplement 1984, ed. C. A. Beichman, G. Neugebauer, H. J. Habing, P. E. Clegg, and T. J. Chester (JPL Pub. D-1855).
Israel, F. P. 1977, *Astr. Ap.*, **60**, 233.
———. 1978, *Astr. Ap.*, **70**, 769.
Keene, J. 1981, *Ap. J.*, **245**, 115.
Leisawitz, D. 1985, Ph.D. thesis, University of Texas at Austin.
Leisawitz, D., Thaddeus, P., and Bash, F. N. 1988, in preparation (LTB).
Lonsdale, C. J., Helou, G., Good, J. C., and Rice, W. 1985, *Cataloged Galaxies and Quasars in the IRAS Survey* (Pasadena: Jet Propulsion Laboratory).
Lonsdale Person, C. J., and Helou, G. 1987, *Ap. J.*, **314**, 513.
Lyngå, G. 1981, Catalog of Open Cluster Data (computer database), NSSDC, Greenbelt, MD.
Lyngå, G. 1982, *Astr. Ap.*, **109**, 213.

Mathis, J. S., Mezger, P. G., and Panagia, N. 1983, *Astr. Ap.*, **128**, 212.
Mermilliod, J.-C. 1976, *Astr. Ap. Suppl.*, **24**, 159.
Mezger, P. G. 1978, *Astr. Ap.*, **70**, 565.
Mezger, P. G., Mathis, J. S., and Panagia, N. 1982, *Astr. Ap.*, **105**, 372.
Mezger, P. G., and Smith, L. F. 1977, in *IAU Symposium 75, Star Formation*, ed. T. de Jong and A. Maeder (Dordrecht: Reidel), p. 133.
Mezger, P. G., and Wink, J. E. 1975, in H II *Regions and Related Topics*, ed. T. L. Wilson and D. Downes (New York: Springer-Verlag), p. 408.
Moffat, A. F. 1971, *Astr. Ap.*, **13**, 30.
———. 1972, *Astr. Ap. Suppl.*, **7**, 355.
Moffat, A. F. J., FitzGerald, M. P., and Jackson, P. D. 1979, *Ap. J. Suppl.*, **38**, 197.
Münch, G. 1952, *Ap. J.*, **116**, 575.
Natta, A., and Panagia, N. 1976, *Astr. Ap.*, **50**, 191.
Panagia, N. 1973, *A.J.*, **78**, 929.
Reich, W. 1982, *Astr. Ap. Suppl.*, **48**, 219.
Reynolds, R. J. 1984, *Ap. J.*, **282**, 191.
Reynolds, R. J., and Ogden, P. M. 1982, *A.J.*, **87**, 306.
Roger, R. S., and Pedlar, A. 1981, *Astr. Ap.*, **94**, 238.
Ryter, C. E., and Puget, J.-L. 1977, *Ap. J.*, **215**, 775.
Savage, B. D., and Mathis, J. S. 1979, *Ann. Rev. Astr. Ap.*, **17**, 73.
Sodroski, T. J., Dwek, E., Hauser, M. G., and Kerr, F. J. 1987, *Ap. J.*, **322**, 101.
Soifer, B. T., Houck, J. R., and Neugebauer, G. 1987, *Ann. Rev. Astr. Ap.*, **25**, 187.
Spitzer, L. 1978, *Physical Processes in the Interstellar Medium* (New York: Wiley).
Torres-Peimbert, S., Lazcano-Araujo, A., and Peimbert, M. 1974, *Ap. J.*, **191**, 401.
Vallee, J. P., Hughes, V. A., and Viner, M. R. 1979, *Astr. Ap.*, **80**, 186.
Walker, G. A. H., and Hodge, S. M. 1968, *Pub. A.S.P.*, **80**, 290.
White, R. L. 1979, *Ap. J.*, **229**, 954.
Wilking, B. A., Harvey, P. M., Lada, C. J., Joy, M., and Doering, C. R. 1984, *Ap. J.*, **279**, 291.
Wramdemark, S. 1982, *Rep. Obs. Lund*, **18**, 63.

M. G. HAUSER and D. LEISAWITZ: NASA Goddard Space Flight Center, Laboratory for Astronomy and Solar Physics, Code 685, Greenbelt, MD 20771